ACTA FACULTATIS
MEDICAE NAISSENSIS

UDC: 615.283:616.936
DOI: 10.5937/afmnai39-31499

Original article

Running title: Repurposing Cipargamin as an Agent Targeting Human Adenosine Receptor A3 in Infected Erythrocytes

Cipargamin Could Inhibit Human Adenosine Receptor A3 with Higher Binding Affinity than *Plasmodium falciparum* P-type ATPase 4: An *In Silico* Study

Toluwase Hezekiah Fatoki[1], Oladoja Abosede Awofisayo[2], and Bolanle Christianah Faleye[3]

[1]*Department of Biochemistry, Federal University Oye-Ekiti, PMB 373, Oye-Ekiti, Ekiti State, Nigeria*
[2]*Department of Pharmaceutical and Medicinal Chemistry, University of Uyo, PMB 1017 Uyo, Nigeria*
[3]*Department of Chemical Science, Joseph Ayo Babalola University, Ikeji-Arakeji, PMB 5006, Ilesa Osun State, Nigeria*

SUMMARY

Aim: This study aimed to predict the molecular targets of cipargamin in humans and estimate the structural dynamics and binding affinity of their interactions compared to that of *Plasmodium falciparum* P-type ATPase 4 (PfATP4).
Methods: In silico methods were used in this study which include target prediction, structure modeling and dynamics, and molecular docking.
Results: The results showed that cipargamin had 100% probability of binding to the human adenosine A3 receptor (ADORA3) and about 15% for other human targets which include tyrosine-protein kinase JAK2, adenosine A2a receptor, phosphodiesterase 5A and cathepsin K. The results of molecular docking showed that binding energy of cipargamin to PfATP4 and hADORA3 were -12.40 kcal/mol^{-1} and -13.40 kcal/mol^{-1} respectively. The docking was validated by the binding of enprofylline and fostamatinib to PfATP4 and hADORA3. Overall, the binding of cipargamin was closely similar to that of fostamatinib. This study shows the potential of cipargamin to modulate the activities of PfATP4 of the parasite (*P. falciparum*) as well as ADORA3 of the host (Homo sapiens).
Conclusion: All the previous studies of cirpagamin have not implicated its action on hADORA3, thus this study provides an insight into a possible role of hADORA3 in the mechanism of malarial infection.

Keywords: **cipargamin, KAE609, PfATP4, ADORA3, malaria, anti-inflammatory, structural modelling and dynamics**

Corresponding author:
Toluwase Hezekiah Fatoki
e-mail: hezekiahfatoki@gmail.com, toluwase.fatoki@fuoye.edu.ng

INTRODUCTION

In 2020, the World Health Organization (WHO) has reported that malaria, a vector-borne infectious disease caused by the hematoprotozoan parasite of genus Plasmodium, remains a disease of global health burden with the presence in 73 countries, leading to an estimated 229 million cases and around 409,000 deaths in year 2019. Antimalarial drugs have been the mainstay of control and prophylaxis against malaria, although there is a current effort in the development of vaccine. Few drugs were developed against malaria in the 20th century with the most important being chloroquine and artemisinin. However, the ability of *P. falciparum* to develop resistance to these treatments has threatened their continuing efficacy and raised the importance of combinations as well as development of new drugs and novel targets for the 21st century in order to achieve malaria-free human generation.

In 2010, cipargamin (KAE609 or NITD609), an active spiroindolone derivative compound, was reported for antimalarial activity, killing culture-adapted as well as field isolates of *P. falciparum* and *P. vivax* with an average effective concentration (EC_{50}) of less than 10 nM (1). In 2014, cipargamin was reported for single-dose cure without resistance, at an average inhibitory concentration (IC_{50}) of 550 pM against asexual blood-stage of *P. falciparum* and elimination half-life of about 24 hours in humans (2). In 2016, the therapeutic outcome of cipargamin in patients was found double when compared to artemisinin which is the present global standard antimalarial therapeutant (3).

Studies have shown that cipargamin inhibits the development of gametocyte and oocyst in mosquitoes, with no significant cytotoxicity in mammalian cells (1, 4). A biophysical study revealed that parasites treated with cipargamin exhibit changes in intracellular pH and they are unable to extrude intracellular sodium (5). The inhibition of adenylate and guanyl cyclases prevented the production of cAMP and cGMP by *P. falciparum*, which led to inhibition of cAMP/cGMP-dependent protein kinase A activities (6, 7). A study has shown that rhoptry protein RhopH2 could regulate new permeability pathways induced in the erythrocyte membrane of *P. falciparum* and that these pathways possibly serve as the main route of influx of Na^+ to the infested cell (8).

Moreover, calcium-dependent protein kinase 5 (PfCDPK5; PF3D7_1337800) as well as P-type cation ATPase (PfATP4; PF3D7_1211900) have been reported to be great potential antimalarial drug targets (9, 10). The involvement of PfATP4 as the direct target of many potential antimalarial compounds including cipargamin, has been a point of contention (11). To provide cogent information contributing to this well-thought dispute, this study used *in silico* methods to investigate human molecular targets of cipargamin and evaluated the molecular binding and structural dynamics of PfATP4.

MATERIALS AND METHODS

In silico target prediction

The structure of cipargamin was obtained from PubChem Compound Database (https://pubchem.ncbi.nlm.nih.gov/) in canonical Simplified Molecular Input Line Entry Specification (SMILES) and Structure Data File (SDF) formats. The SMILES was used for Target prediction on SwissTargetPrediction server (http://www.swisstargetprediction.ch/) where *Homo sapiens* was designated as target organism (12).

In silico structural modelling

The protein sequence of PfATP4 (*Plasmodium falciparum* P-type ATPase 4) and most predicted target for cipargamin hADORA3 (*Homo sapiens* Adenosine receptor A3; ADORA3) were obtained from UniProt database (www.uniprot.org) in FASTA format. The three-dimension (3D) structure of these target proteins were not available in the Protein Data Bank (PDB) database. Thus, their protein sequences (UniProt ID: Q9U445 for PfATP4, and UniProt ID: P0DMS8 for hADORA3) were used for structural modelling on Swissmodel server (13), using protein crystal structure with PDB ID: 5MPM as template for Q9U445 (14), and crystal structure of the human adenosine A1 receptor with PDB ID: 5UEN as template for P0DMS8 (15).

In silico structural dynamics

The modelled structures of PfATP4 and hADORA3 were fixed using PDBFixer implemented in OpenMM v7.3, on CPU platform (16). The protein was then subjected to fast structural flexibility simulation on CAB-flex 2.0 server at default settings (17). The cluster of model structures, contact map

and root-mean square fluctuation (RMSF) of the residues were obtained.

Molecular docking studies

The blind molecular docking studies were carried out on Blind Docking server (18). Enprofylline (DrugBank ID: DB00824 (APRD00273)) and Fostamatinib (DrugBank ID: DB12010) are inhibitors of hADORA3 and thus they were used as ligands to compare and validate the binding of cipargamin. The structure of cipargamin, enprofylline and fostamatinib were retrieved from PubChem Compound Database in Structure Data File (SDF) format. Files were converted from SDF to PDB by using the PyMol software. Docking was initiated on Blind Docking Server, by uploading the target proteins (modelled structures of PfATP4 and hADORA3) and ligands (Cipargamin, Enprofylline and Fostamatinib) in pdb format. The docking simulations of the ligands with target proteins were run at default settings. The binding energies distribution, cluster populations, ligand-protein interactions, and energetic contribution to binding of the ligand-protein complexes were obtained as the docking outputs. The result protein-ligand interaction was visualized and profiled (19, 20).

RESULTS

The results showed that cipargamin bound to Adenosine A3 receptor (ADORA3) with an 100% probability and about 15% for other human targets which include tyrosine-protein kinase JAK2, adenosine A2a receptor, phosphodiesterase 5A and cathepsin K (Table 1).

The QMEAN and GMQE of structural model were -4.94 and 0.52 for PfATP4 as well as -3.18 and 0.76 for hADORA3. The sequence identity of PfATP4 and hADORA3 to their respective template protein were 29.32% and 49.50% (Table 2). Structural flexibility simulation of PfATP4 showed a wide range of amino acid residue fluctuation with highest root-mean-square fluctuation (RMSF) of 7.115 Armstrong (Å) at residue 636 followed by residue 804 (5.472Å), 516 (4.920Å) and others, whereas fluctuations of hADORA3 were found in 7 clusters of amino acid residues with highest RMSF of 3.881Å at residue 213 followed by residue 155 (3.038Å), 158 (2.752Å), 258 (2.273Å) and others (Figure 1 and 2).

Table 1. *Predicted targets in humans with percentage probability of cipargamin binding*

S.No	TARGET			CIPARGAMIN
	Name	Gene ID	UniProt ID	% probability
1	Adenosine A3 receptor	ADORA3	P0DMS8	100
2	Tyrosine-protein kinase JAK2	JAK2	O60674	15
3	Adenosine A2a receptor	ADORA2A	P29274	15
4	Phosphodiesterase 5A	PDE5A	O76074	15
5	c-Jun N-terminal kinase 1	MAPK8	P45983	15
6	Beta-secretase 1	BACE1	P56817	15
7	Gamma-secretase	PSEN2 PSENEN NCSTN APH1A PSEN1 APH1B	P49810 Q9NZ42 Q92542 Q96BI3 P49768 Q8WW43	15
8	Cathepsin K	CTSK	P43235	15
9	Hepatocyte growth factor receptor	MET	P0858	15
10	11-beta-hydroxysteroid dehydrogenase 1	HSD11B1	P28845	15
11	Ribosomal protein S6 kinase 1	RPS6KB1	P23443	15
12	Serine/threonine-protein kinase Aurora-A	AURKA	O14965	15
13	Nitric-oxide synthase, brain	NOS1	P29475	15
14	Epidermal growth factor receptor erbB1	EGFR	P00533	15
15	Rho-associated protein kinase 1	ROCK1	Q13464	15

Table 2: *Structural modelling result*

Target	UniProtKB	Template	Seq Identity	Oligo-state	QSQE	Found by	Method
PfATP4	Q9U445	5mpm.1.A	29.32	monomer	0.00	HHblits	X-ray
hADORA3	P0DMS8	5uen.1.A	49.50	homo-dimer	0.23	HHblits	X-ray

Resolution	Seq Similarity	Range	Coverage	Description	GMQE	QMEAN
3.30Å	0.34	117 - 1257	0.76	Sarcoplasmic /endoplasmic reticulum calcium ATPase 2	0.52	-4.94
3.20Å	0.43	7 - 305	0.95	Adenosine receptor A1	0.76	-3.18

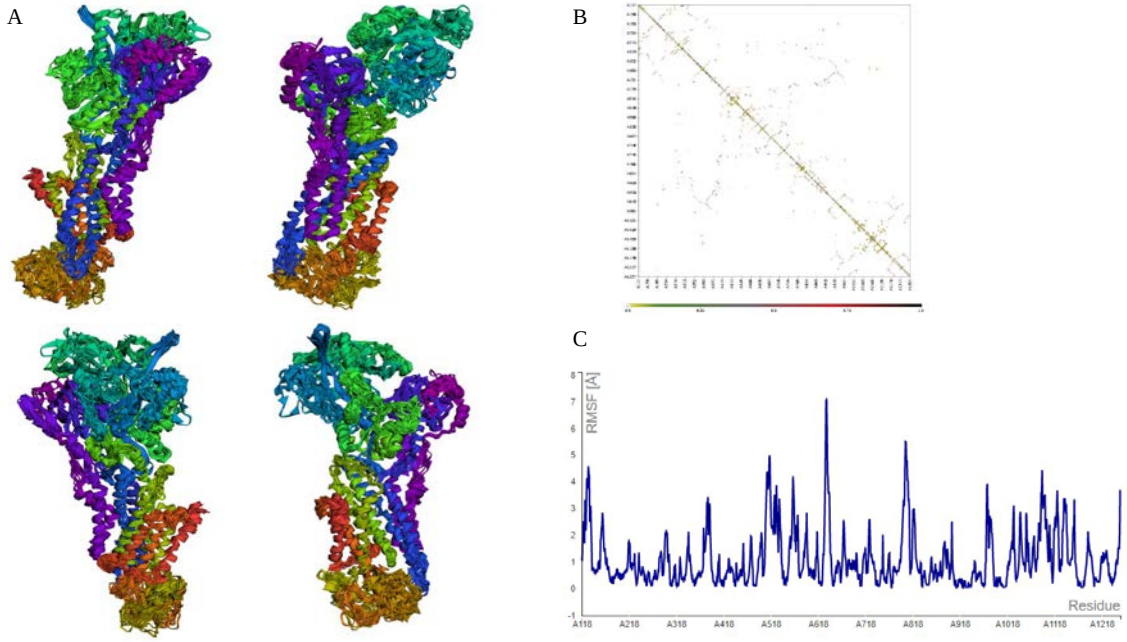

Figure 1. *Structural flexibility dynamics of PfATP4 (A) Cluster of 10 model structures; (B) Contact map; (C) Fluctuation plot*

The results of molecular docking (Figure 3 - 8) showed the binding energy of (1) cipargamin to PfATP4 and hADORA3 as -12.40 kcal mol^{-1} and -13.40 kcal mol^{-1} respectively (Figure 3 and 4); (2) Enprofylline to PfATP4 and hADORA3 as -7.70 kcal mol^{-1} and -6.70 kcal mol^{-1}, respectively (Figure 5 and 6); and (3) Fostamatinib to PfATP4 and hADORA3 as -12.00 kcal mol^{-1} and -11.00 kcal mol^{-1}, respectively (Figure 7 and 8). The binding of cipargamin and fostamatinib increased down the PfATP4 gradient while that of enprofylline decreased down the PfATP4 gradient (Figure 9). Overall, the binding of cipargamin is similar to that of fostamatinib.

The amino acid residues involved in the binding of (1) cipargamin with PfATP4 are ILE378, PRO384, ASN1082, GLU1084, ARG1113, and ASP1116; (2) enprofylline with PfATP4 are ASN155, ILE157, SER230, SER246, ILE263, ALA309, THR310, and VAL331; (3) fostamatinib with PfATP4 are TRP1071, TRP1078, GLY1128, CYS1130, ARG1131, LYS1133, ASN1135, LYS1136, SER1138 and GLU1144; (4) cipargamin and hADORA3 are PHE168, LEU246, and ASN250; (5) enprofylline and hADORA3 are THR94, TYR176, SER181 and TRP243; (6) fostamatinib and hADORA3 are LEU90, LEU91, THR94, PHE168, TRP243 and HIS272.

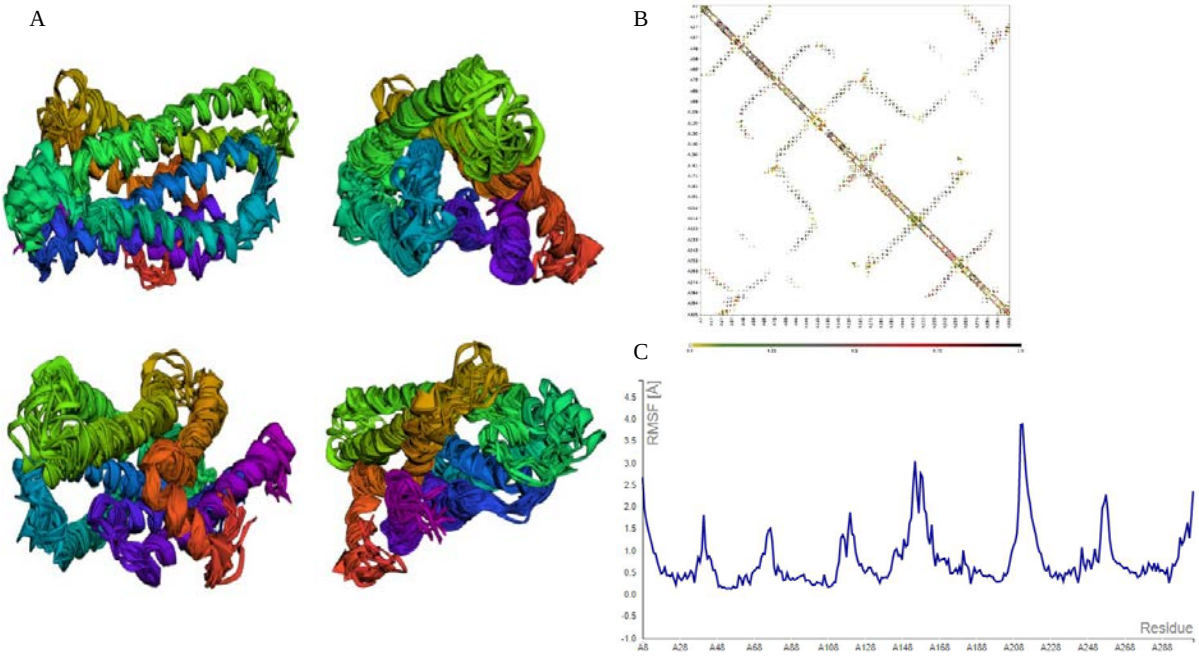

Figure 2. *Structural flexibility dynamics of hADORA3 (A) Cluster of 10 model structures; (B) Contact map; (C) Fluctuation plot*

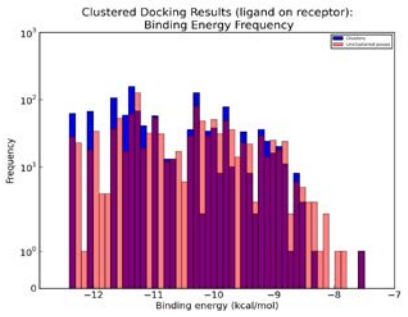

Binding energy (kcal/mol)	Poses in cluster	Best pose	Binding site coordinates
-12.40	62	269	(-30.87, -13.18, -38.16)
-12.10	67	1011	(-42.67, -25.51, -47.71)
-11.70	107	294	(-18.73, 17.65, -50.24)
-11.50	59	452	(2.47, 65.53, -79.45)
-11.40	79	781	(-7.22, 56.66, -59.43)
-11.40	53	186	(-9.97, 62.79, -39.26)
-11.40	25	832	(-22.81, -2.96, -48.98)
-11.30	68	668	(-13.46, 67.55, -61.80)
-11.20	41	321	(-10.37, 38.70, -51.24)
-11.00	57	1087	(-33.46, 7.90, -75.65)
-10.80	13	973	(-46.04, -17.31, -43.67)
-10.70	13	836	(-27.80, -9.12, -44.95)
-10.40	36	495	(-8.21, 76.07, -63.59)
-10.30	32	117	(10.20, 62.06, -49.86)

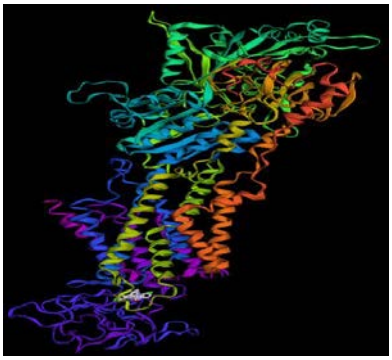

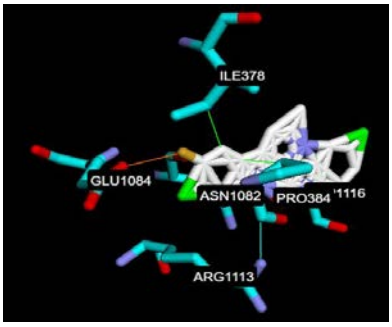

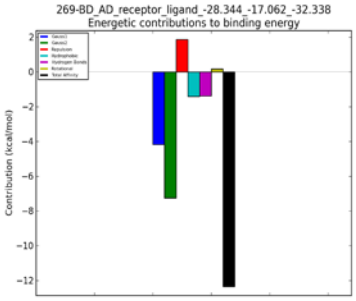

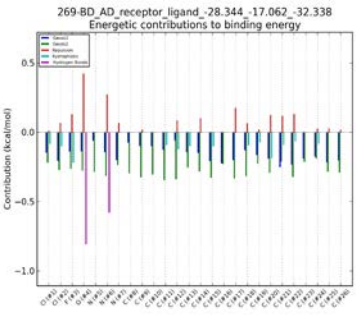

Figure 3. *Cipargamin docking to PfATP4 showing binding interaction and energetics of Cluster #1 (-12.40 kcal.mol^{-1})*

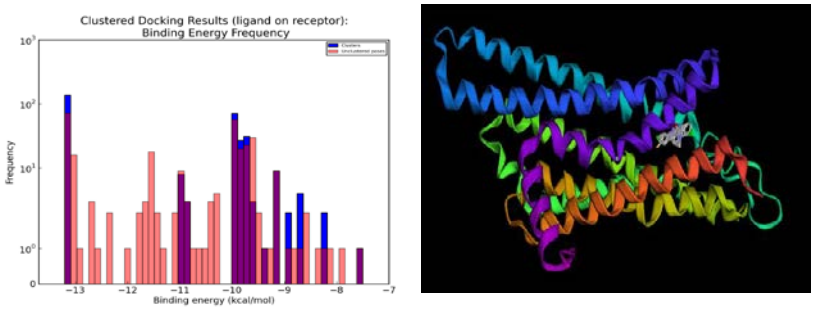

Binding energy (kcal/mol)	Poses in cluster	Best pose	Binding site coordinates
-13.20	137	256	(53.17, 59.06, 140.81)
-11.00	8	1	(59.59, 60.56, 154.91)
-10.90	3	14	(56.07, 53.51, 144.69)
-9.90	32	185	(25.13, 73.69, 143.77)
-9.90	39	101	(19.19, 57.79, 148.11)
-9.80	27	294	(33.81, 52.89, 157.22)
-9.70	31	115	(27.81, 55.25, 130.54)
-9.60	3	48	(27.73, 44.17, 139.61)
-9.40	1	109	(17.90, 50.36, 138.26)
-9.20	9	205	(11.00, 74.33, 146.84)
-8.90	2	147	(61.59, 65.62, 130.35)
-8.70	4	150	(61.80, 54.65, 124.30)
-8.20	2	151	(72.23, 53.00, 136.18)
-7.50	1	298	(24.95, 46.89, 166.38)

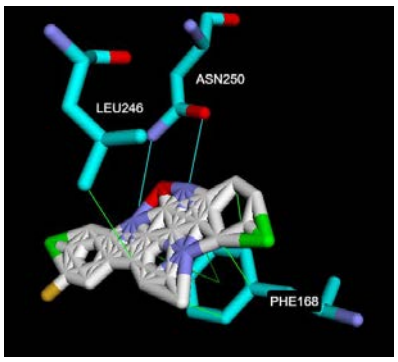

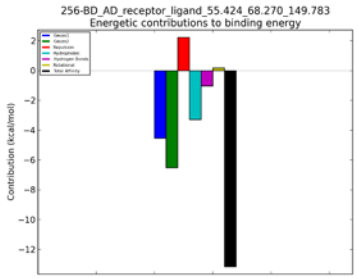

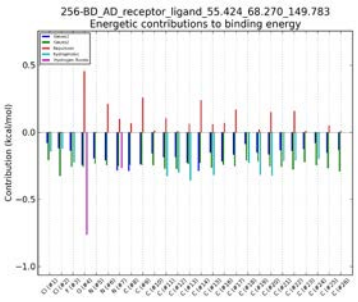

Figure 4. *Cipargamin docking to hADORA3 showing binding interaction and energetics of Cluster #1 (-13.20 kcal.mol^{-1})*

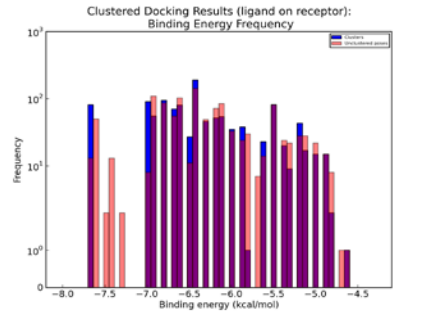

Binding energy (kcal/mol)	Poses in cluster	Best pose	Binding site coordinates
-7.70	81	150	(1.49, 56.52, -45.50)
-7.00	90	970	(-40.80, -26.17, -48.01)
-6.90	55	4	(-8.77, 63.57, -40.26)
-6.80	95	838	(-23.20, -2.07, -48.68)
-6.70	70	742	(-32.49, 34.23, -65.00)
-6.60	55	446	(2.99, 65.95, -78.35)
-6.60	25	1109	(-34.23, -16.16, -54.40)
-6.50	27	1116	(-31.64, 4.38, -59.01)
-6.40	64	160	(3.21, 78.93, -66.94)
-6.40	68	100	(-13.42, 39.15, -53.08)
-6.40	33	815	(-39.65, 18.19, -62.88)
-6.40	25	885	(-44.36, 9.23, -61.63)
-6.30	46	169	(-12.05, 64.91, -64.20)
-6.20	25	538	(-5.61, 75.85, -65.21)

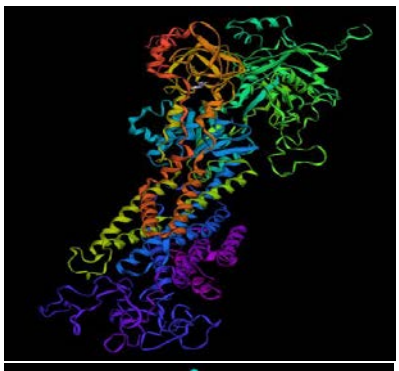

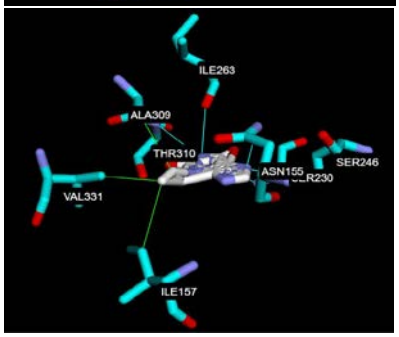

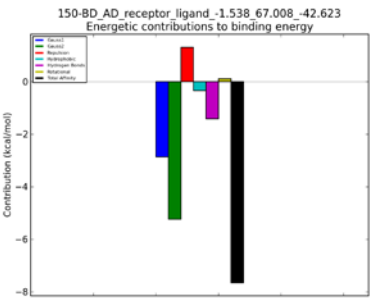

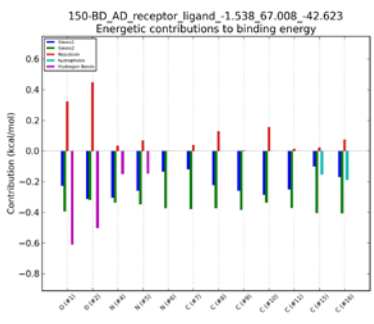

Figure 5. *Enprofylline docking to PfATP4 showing binding interaction and energetics of Cluster #1 (-7.70 kcal.mol^{-1})*

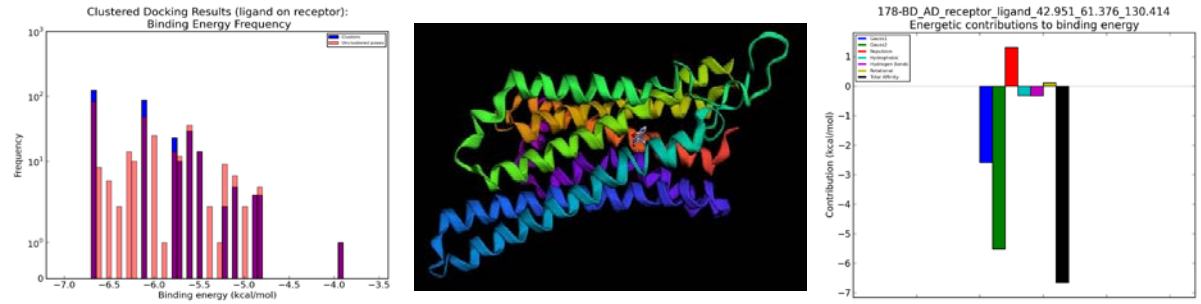

Binding energy (kcal/mol)	Poses in cluster	Best pose	Binding site coordinates
-6.70	123	178	(46.65, 58.07, 135.44)
-6.10	33	12	(55.09, 51.49, 143.71)
-6.10	54	36	(19.02, 50.03, 136.16)
-5.80	23	21	(31.02, 51.56, 154.95)
-5.70	10	190	(25.50, 54.82, 131.11)
-5.60	29	274	(18.91, 58.04, 146.49)
-5.50	8	4	(58.03, 60.88, 155.08)
-5.50	1	147	(54.84, 59.87, 141.55)
-5.50	5	208	(14.37, 57.68, 138.01)
-5.20	2	146	(61.49, 63.84, 131.79)
-5.10	4	151	(74.54, 48.24, 135.81)
-4.90	3	199	(25.88, 72.98, 144.53)
-4.80	3	204	(10.50, 72.52, 147.52)
-3.90	1	298	(25.61, 46.85, 166.09)

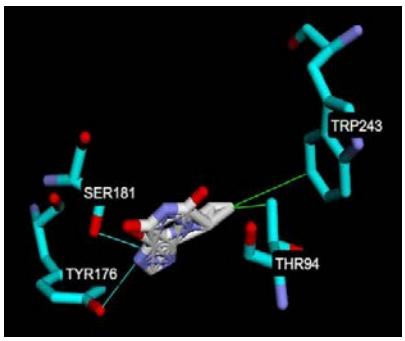

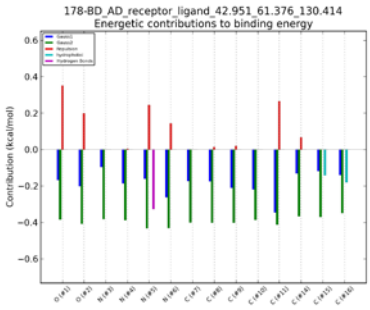

Figure 6. *Enprofylline docking to hADORA3 showing binding interaction and energetics of Cluster #1 (-6.70 kcal.mol^{-1})*

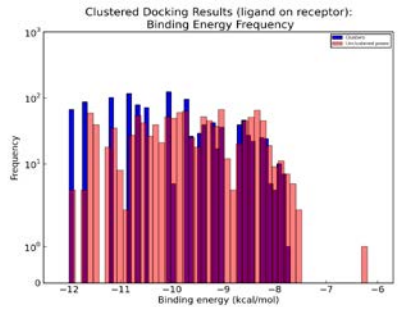

Binding energy (kcal/mol)	Poses in cluster	Best pose	Binding site coordinates
-12.00	66	960	(-44.86, -25.18, -50.75)
-11.70	87	296	(-20.70, 18.14, -50.45)
-11.20	101	170	(-13.87, 68.64, -60.62)
-10.80	62	196	(-5.77, 57.46, -59.69)
-10.80	54	218	(-10.37, 39.30, -49.53)
-10.70	78	268	(-29.45, -9.74, -42.19)
-10.50	71	855	(-34.82, 29.61, -66.85)
-10.10	33	468	(0.93, 64.80, -83.23)
-10.10	76	533	(-1.70, 89.09, -84.32)
-10.10	14	451	(-11.39, 52.07, -75.16)
-10.00	5	630	(-9.72, 76.94, -63.64)
-9.70	29	618	(3.94, 77.72, -62.66)
-9.70	50	672	(-21.83, 62.33, -77.01)
-9.70	9	973	(-40.08, -7.74, -36.90)

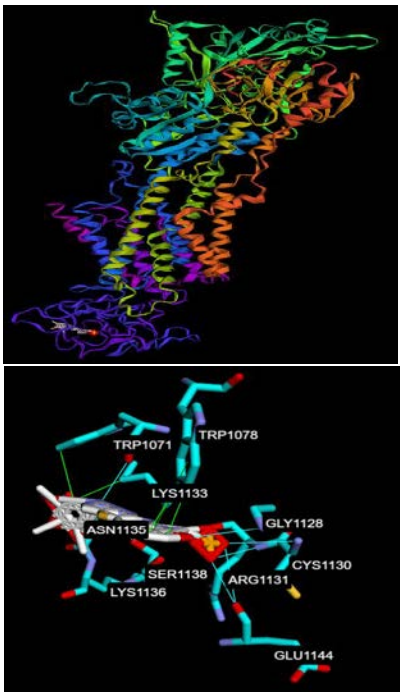

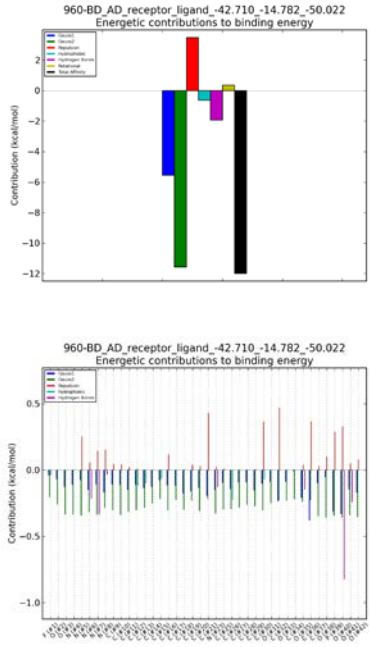

Figure 7. *Fostamatinib docking to PfATP4 showing binding interaction and energetics of Cluster #1 (-12.00 kcal.mol^{-1})*

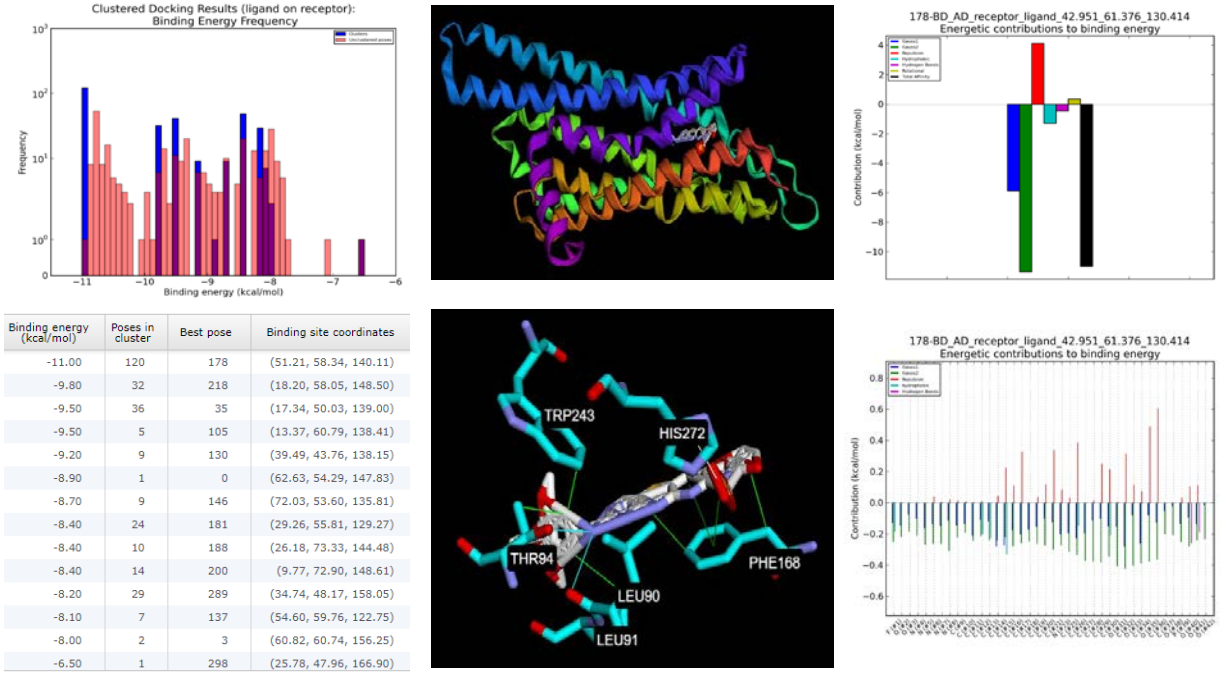

Binding energy (kcal/mol)	Poses in cluster	Best pose	Binding site coordinates
-11.00	120	178	(51.21, 58.34, 140.11)
-9.80	32	218	(18.20, 58.05, 148.50)
-9.50	36	35	(17.34, 50.03, 139.00)
-9.50	5	105	(13.37, 60.79, 138.41)
-9.20	9	130	(39.49, 43.76, 138.15)
-8.90	1	0	(62.63, 54.29, 147.83)
-8.70	9	146	(72.03, 53.60, 135.81)
-8.40	24	181	(29.26, 55.81, 129.27)
-8.40	10	188	(26.18, 73.33, 144.48)
-8.40	14	200	(9.77, 72.90, 148.61)
-8.20	29	289	(34.74, 48.17, 158.05)
-8.10	7	137	(54.60, 59.76, 122.75)
-8.00	2	3	(60.82, 60.74, 156.25)
-6.50	1	298	(25.78, 47.96, 166.90)

Figure 8. *Fostamatinib docking to hADORA3 showing binding interaction and energetics of Cluster #1 (-11.00 kcal.mol^{-1})*

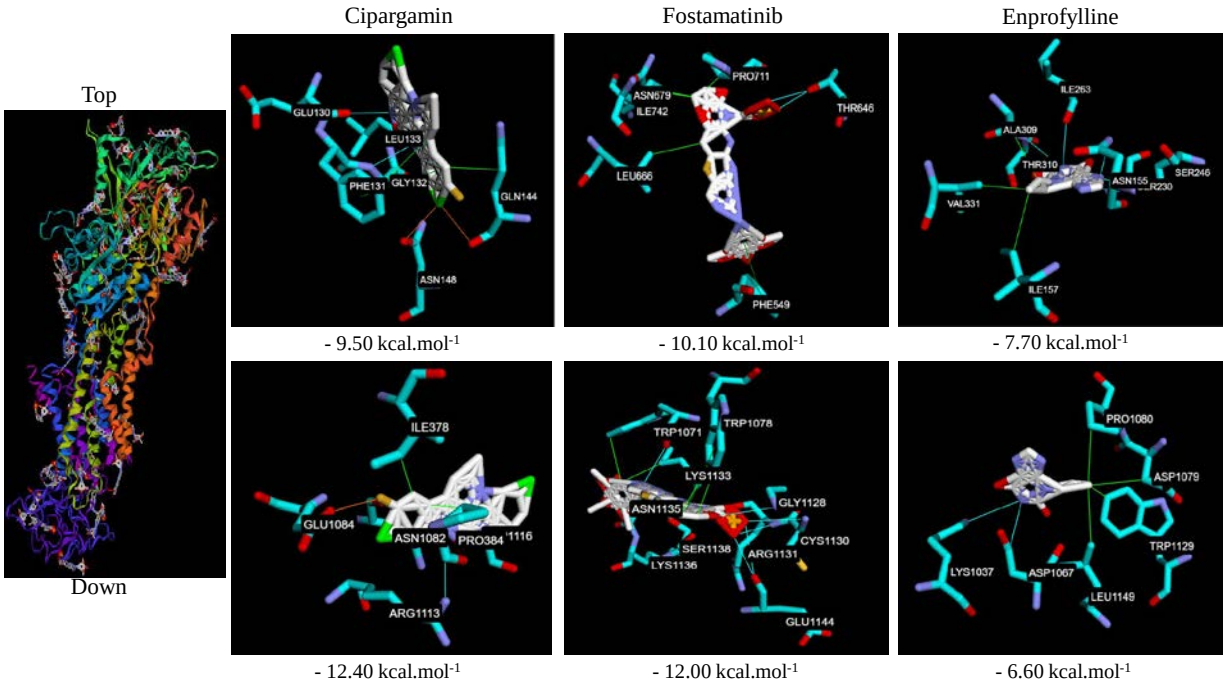

Figure 9. *Highest binding interaction of cipargamin, fostamatinib and enprofylline to the top and down cavity of PfATP4*

DISCUSSION

The QMEAN is used to provide global and local absolute quality estimates of a single model structure based on various geometric properties (21) and it shows the estimated degree of undeviating structural features observed in comparison to that of experimental structures of similar size (22). The QMEAN score for highest quality model structure is greater than or equal to -4.0. The resulting GMQE score reveals the reliability of the alignment of the model with the template sequence, and it ranges between 0 and 1, where the best reliability is equal to 1. Protein dynamics is central to all biological events which include bio-catalysis, signal transduction and cellular regulation (23). The structural dynamics of a protein describes the possible functions it will perform in the biological system. To overcome the complexity involved in the experimental study of protein flexibility, nowadays computational methods are used to simulate the proteins based on validated dataset from existing experiments (17).

PfATP4 gene is expressed at all stages of *P. falciparum* asexual erythrocytic cycle (1), and found as the component of the plasma membrane (1, 24). Malaria is often associated with hyponatremia in the host. The increased influx of sodium ion (Na^+) in a Plasmodium infected erythrocyte causes an upsurge in Na^+ concentration in the erythrocyte cytosol, and triggers the Na^+/K^+ ATPase with two-fold activity in order to maintain a low erythrocytic Na^+ concentration (25). The conservation of a low cytosolic [Na^+] is interrupted by the P-type cation-ATPase inhibitors and that PfATP4 encoded by *P. falciparum* (26, 27) is involved in the active efflux of Na^+ from the parasite (5).

The parasite-induced permeability pathway which has been described as an (unknown) endogenous pathways for the influx of Na^+ in the host cytosol (11) could be via human ADORA3 (hADORA3), in that it matches the unique and explainable target for this compound. hADORA3 belongs to the family member of G protein-coupled receptors (GPCRs) which could be triggered by adenosine (28). hADORA3 gene is located on chromosome 1p13.3 and encodes a protein that consists of 318 amino acids, which is located in the cell membrane. Based on gene ontology, the biological process of ADORA3 includes inflammatory response; activation of adenylate cyclase activity; negative regulations of cell migration, cell population proliferation and NF-kappaB transcription factor activity, and regulation of heart contraction. Copious amounts of hADORA3 gene are expressed in the lung, liver, and immune cells (29), but moderate amounts are expressed in the brain, heart, and other tissues (30). Pharmaceutically, hADORA3 agonists have good therapeutic prospect as anticancer, anti-inflammatory, and cardioprotective agents (31, 32), with several of them at the clinical trial stage of drug development (2, 33). At the cellular level, hADORA3 activation leads to adenylate cyclase (AC) inhibition to reduce cytosolic cyclic AMP (cAMP) levels via the inhibitory guanine nucleotide-binding protein (Gi protein).

In molecular docking, the binding energies that are higher than -5.0 are good indication of affinity of the ligand to the target enzyme or receptor. This study showed that Trp243 and His272 were implicated in the binding of fostamatinib to hADORA3. It has been reported that residue D58, W243 and H272 were conserved in hADORA3 protein, and that H272 could directly or indirectly involve in the coordination of Na^+ (28). The residue W243 plays a critical role in hADORA3 activation, and an experiment has shown that W243A/F mutations reduced agonist-mediated receptor activation without disturbing agonist binding (34) and significant changes were observed in agonist effectiveness and signaling prejudice for the W243F hADORA3 mutant (35). hADORA3 is a multi-pass plasma membrane protein that is modulated by few chemical compounds which include aminophylline (DB01223), enprofylline (DB00824), fostamatinib (DB12010) and piclidenoson (DB05511).

Piclidenoson is indicated as an anti-inflammatory compound which is used to for the treatment of rheumatoid arthritis. Piclidenoson operates as an antagonist of hADORA3. In normal tissues, there is low hADORA3 expression but extreme expression and overexpression have been observed in inflammatory cells and peripheral blood mononuclear cells, respectively (36). hADORA3 deactivation by a specific antagonist often regulates the NF-kappaB signaling pathway in inflammatory cells and initiates immunocompetency effects. Enprofylline is a synthetic dimethylxanthine derivative compound which is structurally associated to caffeine and theophylline. Enprofylline inhibits hADORA3 and phosphodiesterase in erythrocytes, and prevent deformity of the membrane of erythrocytes. Enprofylline also alters the viscosity of the blood by decreasing the

concentration of plasma fibrinogen and raising the fibrinolytic activity (37).

Aminophylline is the ethylenediamine salt of theophylline that prevents the degradation of cAMP by inhibiting phosphodiesterase type III and IV. Theophylline acts as a hADORA3 antagonist (38) and blocks transcription of inflammatory genes by triggering histone deacetylase (39). The active metabolite of fostamatinib, called R406, inhibits hADORA3, phosphodiesterase (PDE5), spleen tyrosine kinase (Syk), UDP-glucuronosyltransferase (UGT1A1), cathepsin L, 5-lipoxygenase, fatty acid amide hydrolase, and adenosine or monoamine uptake transporters (40, 41).

The malaria parasite feeds on red blood cells (RBCs) by degrading Hb in an acidic food vacuole to provide required amino acids for the parasite, create sufficient space for parasite growth and help maintain the osmotic integrity of the infected cell (42). The infected erythrocytes are protected from oxidative stress by biomineralization and sequestered of free oxidized heme and H_2O_2 (which are produced from hemoglobin degradation and they are toxic to the parasite) to form hemozoin through the activity of histidine-rich protein HRP2 (43, 44). Adenosine is readily released by RBCs infected by Plasmodium, or after oxidative stress, through the action of ectonucleotidases CD39 and CD73 which are present on RBC surface (45). Inhibition of hADORA3 can deactivate phospholipase C from releasing Ca^{2+} that acts as a second messenger to elicit various cell responses. The mechanism of action of cipargamin would be by inhibition (antagonism) of hADORA3 and PfATP4 in infected erythrocytes, thus preventing the deformity of erythrocyte membrane, trapped oxygen radicals within the infected erythrocyte, and induced programmed cell death, a process called eryptosis (43, 46).

CONCLUSION

This study has shown the possibility of malaria drug cipargamin to modulate the activities of PfATP4 of the parasite (*Plasmodium falciparum*) as well as ADORA3 of the host (*Homo sapiens*). All the previous studies of cirpagamin had not implicated its action on hADORA3, thus this study provided an insight to possible role of hADORA3 in the mechanism of malarial infection. Also, the fact that major inhibitors of hADORA3 have indication as anti-inflammatory drug, cipargamin could be also repurposed for this indication. Further research would be the study of inhibitory kinetics of cipargamin binding to hADORA3.

Declaration of conflicting interest

The author declares that there is no conflict of interest.

Funding

This work received no funding.

References

1. Rottmann M, McNamara C, Yeung BKS, et al. Spiroindolones, a potent compound class for the treatment of malaria. Science 2010; 329:1175-80. https://doi.org/10.1126/science.1193225

2. Leong FJ, Li R, Jain JP, et al. A first-in-human randomized, double-blind, placebo-controlled, single- and multiple-ascending oral dose study of novel antimalarial Spiroindolone KAE609 (Cipargamin) to assess its safety, tolerability, and pharmacokinetics in healthy adult volunteers. Antimicrob. Agents Chemother 2014; 58:6209-14. https://doi.org/10.1128/AAC.03393-14

3. Goldgof GM, Durrant JD, Ottilie S, et al. Comparative chemical genomics reveal that the spiroindolone antimalarial KAE609 (Cipargamin) is a P-type ATPase inhibitor. Sci Rep 2016; 6:27806-18. https://doi.org/10.1038/srep27806

4. van Pelt-Koops JC, Pett HE, Graumans W, et al. The spiroindolone drug candidate NITD609 potently inhibits gametocytogenesis and blocks *Plasmodium falciparum* transmission to anopheles mosquito vector. Antimicrob. Agents Chemother 2012; 56:3544-8. https://doi.org/10.1128/AAC.06377-11

5. Spillman NJ, Allen RJW, McNamara CW, et al. Na^+ regulation in the malaria parasite *Plasmodium falciparum* involves the cation ATPase PfATP4 and is a target of the spiroindolone antimalarials. Cell Host Microbe 2013; 13:227-37. https://doi.org/10.1016/j.chom.2012.12.006

6. Wentzinger L, Bopp S, Tenor H, et al. Cyclic nucleotide-specific phosphodiesterases of *Plasmodium falciparum*: PfPDEalpha, a non-essential cGMP-specific PDE that is an integral membrane protein. Int J Parasitol 2008; 38(14):1625-37 https://doi.org/10.1016/j.ijpara.2008.05.016

7. Howard BL, Harvey KL, Stewart RJ, et al. Identification of potent phosphodiesterase inhibitors that demonstrate cyclic nucleotide-dependent functions in apicomplexan parasites. ACS Chem Biol 2015; 10(4):1145-54 https://doi.org/10.1021/cb501004q

8. Gilson PR, Kumarasingha R, Thompson J, et al. A 4-cyano-3-methylisoquinoline inhibitor of *Plasmodium falciparum* growth targets the sodium efflux pump PfATP4. Sci Rep 2019; 9:10292-306. https://doi.org/10.1038/s41598-019-46500-5

9. Vaidya AB, Morrisey JM, Zhang Z, et al. Pyrazoleamide compounds are potent antimalarials that target Na þ homeostasis in intraerythrocytic *Plasmodium falciparum*. Nat Commun 2014; 5:5521-30. https://doi.org/10.1038/ncomms6521

10. Dvorin JD, Martyn DC, Patel SD, et al. A plant-like kinase in *Plasmodium falciparum* regulates parasite egress from erythrocytes. Science 2010; 328:910-2. https://doi.org/10.1126/science.1188191

11. Spillman, NJ, Kirk, K. The malaria parasite cation ATPase PfATP4 and its role in the mechanism of action of a new arsenal of antimalarial drugs. Int J Parasitol Drugs Drug Resist 2015; 5:149-162. https://doi.org/10.1016/j.ijpddr.2015.07.001

12. Gfeller D, Grosdidier A, Wirth M, et al. SwissTargetPrediction: a web server for target prediction of bioactive small molecules. Nucleic Acids Res 2014; 42(W1):W32-W38. https://doi.org/10.1093/nar/gku293

13. Waterhouse A, Bertoni M, Bienert S, et al. SWISS-MODEL: homology modelling of protein structures and complexes. Nucleic Acids Res 2018; 46(W1):W296-W303. https://doi.org/10.1093/nar/gky427

14. Sitsel A, De Raeymaecker J, Drachmann ND, et al. Structures of the heart specific SERCA2a Ca^{2+}-ATPase. EMBO J 2019; 38(5): e100020. https://doi.org/10.15252/embj.2018100020

15. Glukhova A, Thal DM, Nguyen AT, et al. Structure of the Adenosine A1 Receptor Reveals the Basis for Subtype Selectivity. Cell 2017;168(5):867-877.e13. https://doi.org/10.1016/j.cell.2017.01.042

16. Eastman P, Swails J, Chodera JD, et al. OpenMM 7: Rapid development of high-performance algorithms for molecular dynamics. PLoS Comput Biol 2017; 13(7):e1005659. https://doi.org/10.1371/journal.pcbi.1005659

17. Kuriata A, Gierut AM, Oleniecki T, et al. (2018). CABS-flex 2.0: a web server for fast simulations of flexibility of protein structures. Nucleic Acids Res 2018; 46(W1):W338-43. https://doi.org/10.1093/nar/gky356

18. Sánchez-Linares I, Pérez-Sánchez H, Cecilia JM, García JM. High-throughput parallel blind virtual screening using BINDSURF. BMC Bioinformatics 2012; https://doi.org/10.1186/1471-2105-13-S14-S13

19. Rego N, Koes D. 3Dmol.js: molecular visualization with WebGL, Bioinformatics 2015; 31(8):1322-1324. https://doi.org/10.1093/bioinformatics/btu829

20. Salentin S, Schreiber S, Haupt VJ, Adasme MF, Schroeder M. PLIP: fully automated protein-ligand interaction profiler. Nucl Acids Res 2015; 43(W1):W443-W447. https://doi.org/10.1093/nar/gkv315

21. Studer G, Rempfer C, Waterhouse AM, et al. QMEAND is co - distance constraints applied on model quality estimation. Bioinformatics 2020; 36:1765-71 https://doi.org/10.1093/bioinformatics/btz828

22. Benkert P, Biasini M, Schwede T. Toward the estimation of the absolute quality of individual protein structure models. Bioinformatics 2011; 27:343-50. https://doi.org/10.1093/bioinformatics/btq662

23. Fatoki TH, Ibraheem O, Ogunyemi IO, et al. Network Analysis, Sequence and Structure Dynamics of Key Proteins of Coronavirus and Human Host, and Molecular Docking of Selected Phytochemicals of Nine Medicinal Plants. J Biomol Stru Dynam 2021; 39(16):6195-6217. https://doi.org/10.1080/07391102.2020.1794971

24. Dyer M, Jackson M, McWhinney C, et al. Analysis of a cation-transporting ATPase of *Plasmodium falciparum*. Mol Biochem Parasitol 1996; 78: 1-12. https://doi.org/10.1016/S0166-6851(96)02593-5

25. Staines HM, Ellory JC, Kirk K. Perturbation of the pump-leak balance for Na^+ and K^+ in malaria-infected erythrocytes. Am J Physiol Cell Physiol 2001; 280:C1576-C1587. https://doi.org/10.1152/ajpcell.2001.280.6.C1576

26. Martin RE, Ginsburg H, Kirk K. Membrane transport proteins of the malaria parasite. Mol Microbiol 2009; 74:519-28. https://doi.org/10.1111/j.1365-2958.2009.06863.x

27. Martin RE, Henry RI., Abbey JL, et al. The 'permeome' of the malaria parasite: an overview of the membrane transport proteins of *Plasmodium falciparum*. Genome Biol 2005; 6, R26. https://doi.org/10.1186/gb-2005-6-3-r26

28. Ciancetta A, Rubio P, Lieberman DI, Jacobson KA. A3 adenosine receptor activation mechanisms: molecular dynamics analysis of inactive, active, and fully active states. J Comp Mol Design 2019; 33:983–996 https://doi.org/10.1007/s10822-019-00246-4

29. Linden J. Cloned adenosine A3 receptors: pharmacological properties, species differences and receptor functions. Trends Pharmacol Sci 1994; 15:298-306 https://doi.org/10.1016/0165-6147(94)90011-6

30. Lopes LV, Rebola N, Pinheiro PC, et al. Adenosine A3 receptors are located in neurons of the rat hippocampus. NeuroReport 2003; 14:1645-8 https://doi.org/10.1097/00001756-200308260-00021

31. Jacobson KA, Merighi S, Varani K, et al. A3 adenosine receptors as modulators of

inflammation: from medicinal chemistry to therapy. Med Res Rev 2017; 38:1031-72 https://doi.org/10.1002/med.21456

32. Fishman P, Bar-Yehuda S, Liang BT, Jacobson KA. Pharmacological and therapeutic effects of A3 adenosine receptor agonists. Drug Discov Today 2012; 17:359-66. https://doi.org/10.1016/j.drudis.2011.10.007

33. White NJ, Pukrittayakamee S, Phyo AP, et al. Spiroindolone KAE609 for falciparum and vivax malaria. N Engl J Med 2014; 371: 403-10. https://doi.org/10.1056/NEJMoa1315860

34. Gao Z-G, Chen A, Barak D, et al. Identification by site-directed mutagenesis of residues involved in ligand recognition and activation of the human A3 adenosine receptor. J Biol Chem 2002; 277:19056-63. https://doi.org/10.1074/jbc.M110960200

35. Stoddart LA, Kellam B, Briddon SJ, Hill SJ. Effect of a toggle switch mutation in TM6 of the human adenosine A3 receptor on Gi protein-dependent signalling and Gi-independent receptor internalization. Br J Pharmacol 2014; 171:3827-44 https://doi.org/10.1111/bph.12739

36. Bar-Yehuda S, Silverman MH, Kerns WD, et al. The anti-inflammatory effect of A3 adenosine receptor agonists: a novel targeted therapy for rheumatoid arthritis. Expert Opin Investig Drugs 2007; 16(10):1601-13. https://doi.org/10.1517/13543784.16.10.1601

37. Linden J, Thai T, Figler H, Jin X, Robeva AS. Characterization of human A(2B) adenosine receptors: radioligand binding, western blotting, and coupling to G(q) in human embryonic kidney 293 cells and HMC-1 mast cells. Mol Pharmacol1999, 56(4):705-13.

38. Stella L, de Novellis V, Marabese I, et al. The role of A3 adenosine receptors in central regulation of arterial blood pressure. Br J Pharmacol 1998; 125(3):437-40 https://doi.org/10.1038/sj.bjp.0702126

39. Ito K, Lim S, Caramori G, et al. A molecular mechanism of action of theophylline: Induction of histone deacetylase activity to decrease inflammatory gene expression. Proc Natl Acad Sci 2002; 99(13):8921-6. https://doi.org/10.1073/pnas.132556899

40. Rolf MG, Curwen JO, Veldman-Jones M, et al. In vitro pharmacological profiling of R406 identifies molecular targets underlying the clinical effects of fostamatinib. Pharmacol Res Perspect 2015; 3(5):e00175. https://doi.org/10.1002/prp2.175 https://doi.org/10.1002/prp2.175

41. Braselmann S, Taylor V, Zhao H, et al. R406, an orally available spleen tyrosine kinase inhibitor blocks fc receptor signaling and reduces immune complex-mediated inflammation. J Pharmacol Exp Ther 2006; 319(3):998-1008. https://doi.org/10.1124/jpet.106.109058

42. Lew VL, Tiffert T. Ginsburg H. Excess hemoglobin digestion and the osmotic stability of *Plasmodium falciparum*-infected red blood cells. Blood 2003; 101: 4189-94. https://doi.org/10.1182/blood-2002-08-2654

43. Becker K, Tilley L, Vennerstrom JL, et al. Oxidative stress in malaria parasite-infected erythrocytes: host-parasite interactions. Int J Parasitol 2004; 34, 163-89. https://doi.org/10.1016/j.ijpara.2003.09.011

44. Akompong T, Kadekoppala M, Harrison T, et al. Trans expression of a *Plasmodium falciparum* histidine-rich protein II (HRPII) reveals sorting of soluble proteins in the periphery of the host erythrocyte and disrupts transport to the malarial food vacuole. J Biol Chem 2002; 277, 28923-33. https://doi.org/10.1074/jbc.M201968200

45. Ramdani G, Langsley G. ATP, an Extracellular Signaling Molecule in Red Blood Cells: A Messenger for Malaria? Biomed J 2014; 37:284-92. https://doi.org/10.4103/2319-4170.132910

46. Jimenez-Diaz MB, Ebert D, Salinas Y, et al. (+)-SJ733, a clinical candidate for malaria that acts through ATP4 to induce rapid host-mediated clearance of Plasmodium. Proc Natl Acad Sci U.S.A. 2014; 111(50), E5455-62. https://doi.org/10.1073/pnas.1414221111

Article info

Received: March 24, 2021
Revised: August 24, 2021
Accepted: November 1, 2021

Cipargamin bi mogao da inhibira humani adenozinski receptor A3 sa većim afinitetom vezivanja od parazita *Plasmodium falciparum* P-tipa ATPase 4: *In silico* studija

Toluwase Hezekiah Fatoki[1], Oladoja A. Awofisayo[2], Bolanle Christianah Faleye[3]

[1]*Departman za biohemiju, Federalni univerzitet Oye-Ekiti, PMB 373, Oye-Ekiti, Država Ekiti, Nigerija*
[2]*Departman za farmaceutsku i medicinsku hemiju, Univerzitet Uyo, PMB 1017 Uyo, Nigerija*
[3]*Departman za hemijske nauke, Univerzitet Joseph Ayo Babalola, Ikeji-Arakeji, PMB 5006, Ilesa Država Osun, Nigerija*

SAŽETAK

Cilj. Cilj studije bilo je predviđanje molekularnih meta cipargamina kod ljudi, kao i procena strukturalne dinamike i afiniteta vezivanja njihovih interakcija u poređenju sa parazitom *Plasmodium falciparum* P-tipa ATPase 4 (PfATP4).

Metode. U studiji su korišćene *in silico* metode koje uključuju predviđanje mete, modelovanje strukture i dinamike i molekularno pristajanje. Rezultati su pokazali to da je cipargamin imao stoprocentnu mogućnost vezivanja za humani Adenosine A3 receptor (ADORA3) i oko 15% mogućnosti vezivanja za druge humane mete, koje uključuju protein tirozin kinazu JAK2, adenozin A2a receptor, fosfodiasterazu 5A i katepsin K.

Rezultati . Rezultati molekularnog pristajanja pokazali su to da je energija vezivanja cipargamina za PfATP4 iznosilac -12,40 kcal/mol^{-1}, a energija vezivanja za hADORA3 -13,40 kcal/mol^{-1}. Molekularno pristajanje vrednovano je vezivanjem enprofilina za PfATP4 i fostamanitiba za hADORA3. U suštini, vezivanje cipargamina jako je slično vezivanju fostamanitiba. Studija pokazuje potencijal cipargamina da menja aktivnosti PfATP4 parazita, kao ADORA3 domaćina (*Homo sapiens*).

Zaključak. Dosadašnje studije o cipargaminu nisu ukazale na njegovo delovanje na hADORA3, tako da ova studija pruža uvid u moguću ulogu hADORA3 u mehanizmu malarije.

Ključne reči: **cipargamin, KAE609, PfATP4, ADORA3, malarija, antiinflamatorni, strukturalno modelovanje i dinamika**